Graduate Design | White Paper

SIEMENS Gamesa
RENEWABLE ENERGY

University of Colorado Boulder

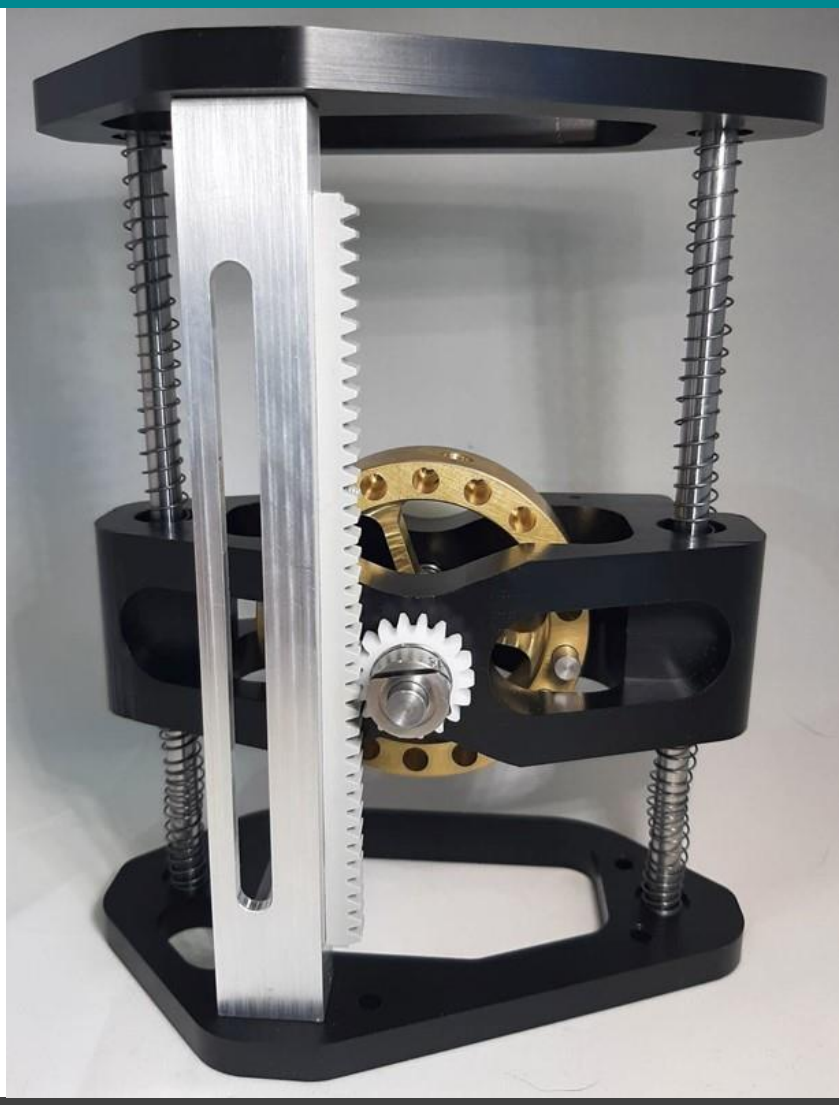

Tunable Oscillating and Rotational Kinematic (TORK) Damper

Jamie Frankel and Ryan Weatherbee

Summary

Wind is rapidly becoming a more prevalent source of energy around the world. Simultaneously, wind turbines are being designed to be larger and more efficient in order to increase their output. As the blades on the turbines get longer, unwanted vibrations can cause extremely high stresses within their structures. Siemens Gamesa Renewable Energy (SGRE) has collaborated with a team of students from the University of Colorado Boulder to create a device that aims to reduce these vibrations.

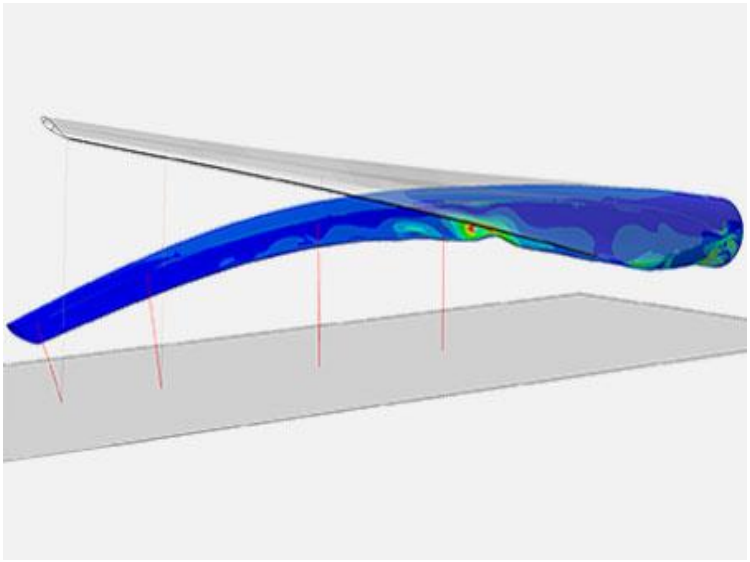

Figure 1: K. Krogh-Jeppesen, "They break turbine blades at Risø - DTU," https://www.dtu.dk, 18-Jan-2016. [Online].

Project Mission

The goal of this project is to successfully design and test a proof-of-concept prototype vibration damper for a cantilevered beam which represents a scaled model of a wind turbine blade. The prototype should add significant damping to the cantilevered beam across a range of frequencies near the first natural frequency of the beam. At the end of the project, a proof-of-concept damping device as well as a test fixture, exciter mechanism, and the associated engineering models will be delivered to SGRE.

Project Specifications

Design requirements for the damping device were put forth by SGRE. The specifications were derived as scaled down targets for a full-size wind turbine blade.

Parameters	***Requirements***
Beam length	2 meters
Weight of device	≤ 5% of beam mass
Logarithmic decrement	≥ 20%
1st mode natural frequency	Between 1 and 3 Hz
Exciter force	Create ± 20% deflection of the beam
Device height	≤ 17 cm
Orientation-free	Functionality regardless of beam orientation

Introduction to Tuned Mass Dampers

One common vibration damper is known as a tuned mass damper (TMD). TMDs are easily scalable and are used in a wide array of applications ranging from cars to skyscrapers. TMDs essentially function by matching the natural frequency of the structure they are attached to but move out of phase. The vibration energy of the structure is transferred to the TMD mass and then dissipated through friction and viscous damping, thus reducing the amplitude of vibration of the structure to an acceptable level. An idealized system model of a TMD is shown in Figure 2. This style of damper inspired the final design of the system described in this report.

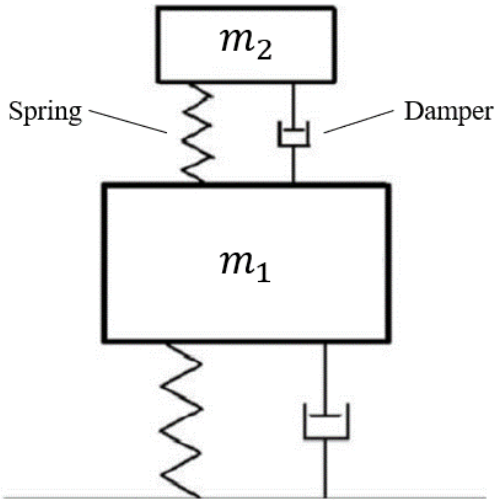

Figure 2: Idealize model of a linear TMD

Idealized Model of the TORK Damper

The Tunable Oscillating and Rotating Kinematic (TORK) Damper is a type of TMD in which the linear motion of the smaller mass is used to rotate a heavy flywheel via a rack and pinion mechanism. This allows the device to have more inertia when compared to a simple TMD of the same mass. Having more inertia allows this device to provide the necessary system damping with less total linear motion when compared to a purely linear TMD. The idealized model of the TORK Damper is shown in Figure 3.

The TORK Damper has a few other notable benefits. First, the system has more design parameters that can be tuned for optimum damping dynamics when compared to a normal TMD. The linear mass, rotational inertia of the flywheel, and the radius of the pinion are all separate parameters that can be changed to tune the system's inertia. The only way to do this with the linear TMD is by changing the mass, m_2. Additionally, the rotational motion allows the device to incorporate a rotary damper (dashpot) to provide the damping coefficient, b_2. Compared to a linear damper, a rotary damper will not constrain the travel distance of the smaller mass.

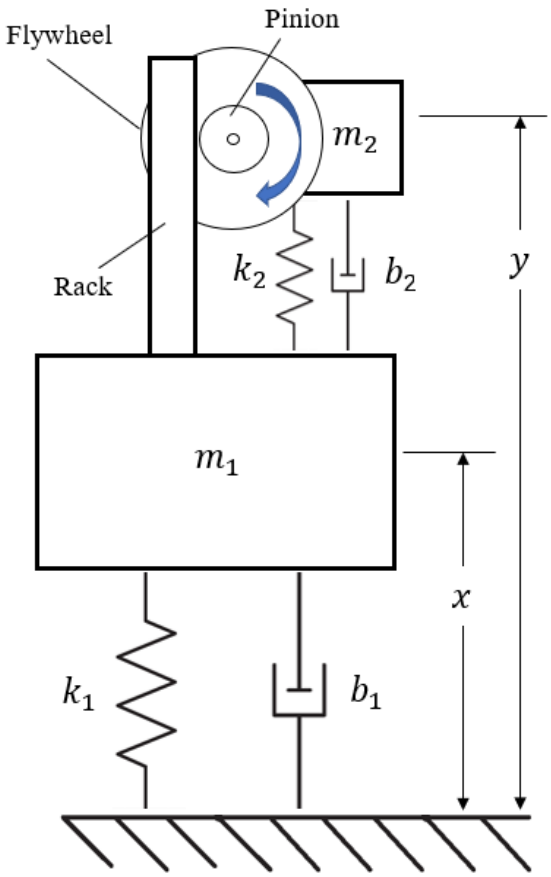

Figure 3: Idealized model of the TORK Damper

From the idealized model of the TORK Damper, a free body diagram can be created for both m_1 and m_2. These free body diagrams are shown in Figure 4. From these free body diagrams, the coupled system of differential equations which describe the dynamics of the idealized TORK Damper can be derived.

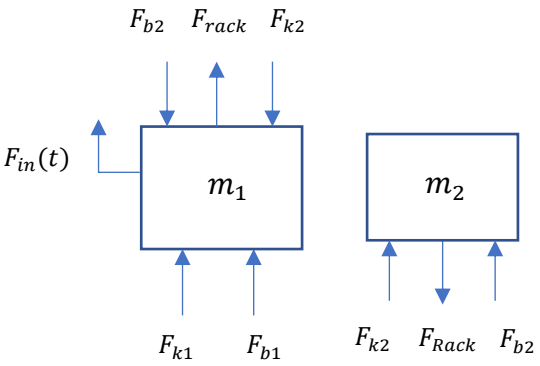

Figure 4: Free body diagrams for the TORK Damper

$$\left(m_2 + m_w + \frac{I}{r^2}\right)\ddot{y} + b_2\dot{y} + k_2 y = \frac{I}{r^2}\ddot{x} + b_2\dot{x} + k_2 x$$

$$\left(m_1 + \frac{I}{r^2}\right)\ddot{x} + (b_1 + b_2)\dot{x} + (k_{1+}k_2)x = \frac{I}{r^2}\ddot{y} + b_2\dot{y} + k_2 y + f_{in}(t)$$

Variable Name	***Represented Parameter***
m_1	Effective beam mass
m_2	Mass of linear components in TORK Damper
m_w	Mass of rotating components in TORK Damper
I	Mass moment of inertia of rotating components
r	Radius of the pinion
k	Spring constants
b	Damping coefficients
$f_{in}(t)$	Input force as a function of time
x	Position of m_1 with respect to ground
y	Position of m_2 with respect to ground

The linear, idealized model has been shown above. In reality, the system has nonlinearities both from friction between the moving components within the TORK Damper and the non-constant damping coefficient from the dashpot. The non-linear system model is simulated with a SIMULINK block diagram shown in Figure 5.

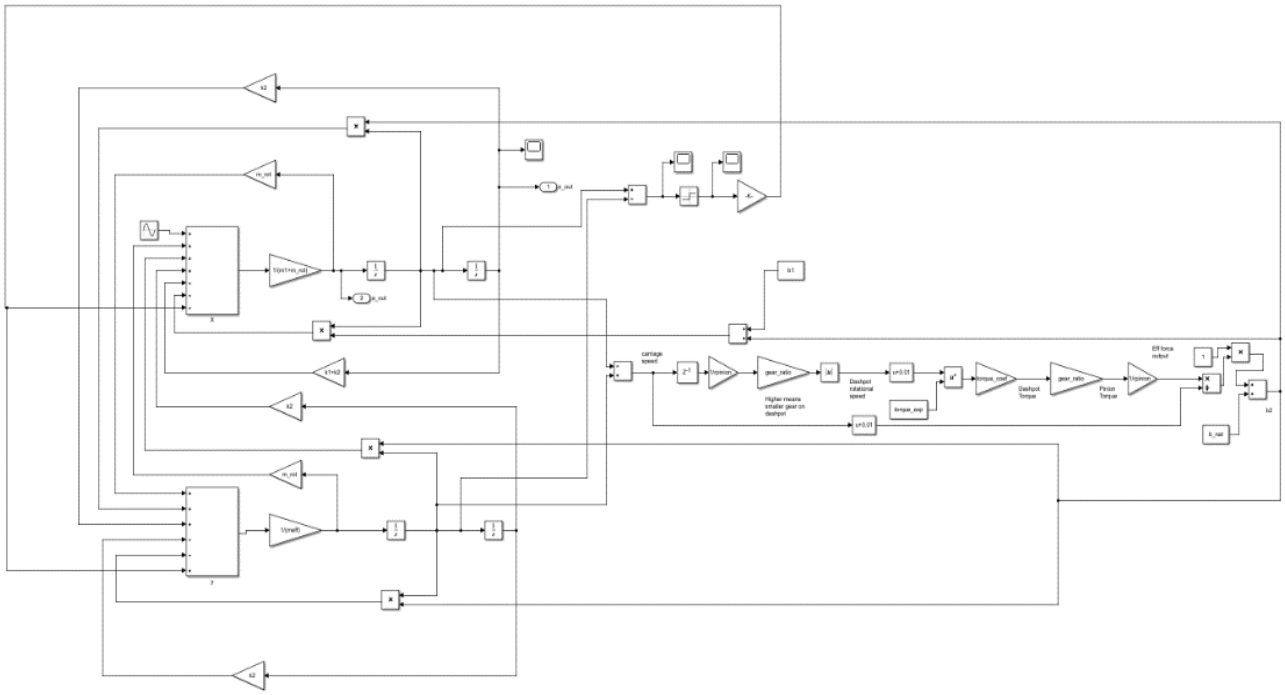

Figure 5: Non-linear Simulink model of the TORK Damper

Design

The TORK Damper, shown in Figure 6, consists of more than 50 components, 21 of which are custom or contain custom features. The most important components in the TORK damper include the carriage, the flywheel, and the springs. These components are described in the following sections.

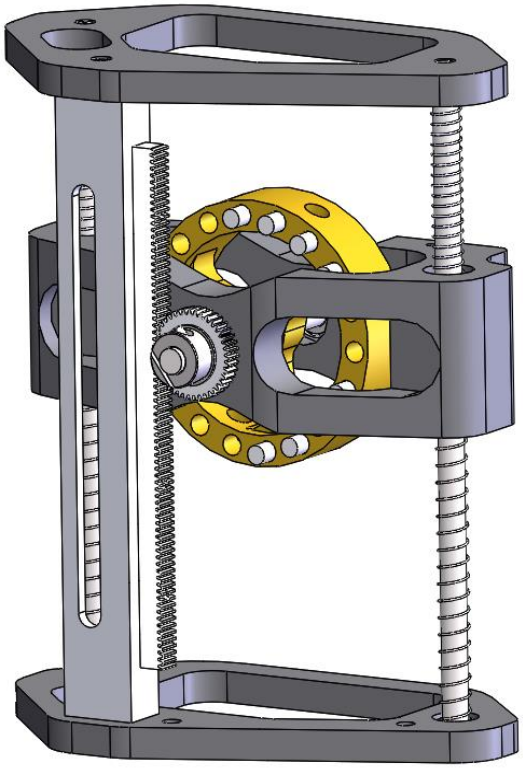

Figure 6: CAD model of the TORK Damper

Carriage

The carriage houses the linear and roller bearings to provide an interface between rotational and linear motion. The design of the carriage was intended to offer dual sided support to the axle and flywheel. The carriage itself is made of Delrin as opposed to more dense materials and includes slots for further mass reduction. Reducing the mass of the carriage is essential as it allows more mass to be allotted to the flywheel. When more mass can be allotted to the flywheel, the overall travel needed to achieve the necessary damping becomes shorter. The machinability of this part was considered, and multiple sets of parallel faces were created to ensure ease of manufacturing.

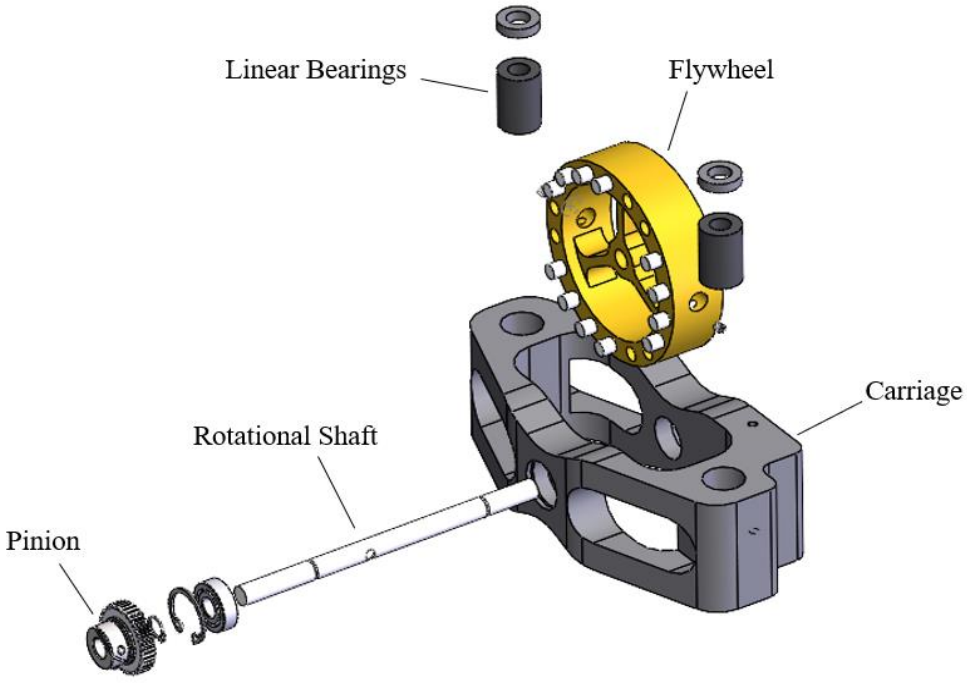

Figure 7: Exploded view of the carriage subassembly

Flywheel

Flywheel design was crucial as the flywheel is the most significant contributor to damping in the TORK Damper; it contributes to both the linear and rotational mass. This part is made of brass as it is denser than steel yet still easily machinable. The flywheel was designed to have as much of the mass as far away from the center as possible. The flywheel was optimized so that the spokes were narrower to allot more mass to the outer ring.

In order to have another tunable parameter within the system, the mass and moment of inertia need to be variable. To design this into the flywheel, threaded holes in a circular pattern were created to house up to 18 tungsten rods. Tungsten rods were chosen as they are significantly denser than the brass of the flywheel. The rods must be placed with rotational symmetry around the flywheel to have a rotationally balanced mass. The system's nominal mass and moment of inertia are designed with 12 tungsten rods installed in the flywheel. To tune the mass and moment of inertia to account for any discrepancies in the system after construction, up to six additional rods can be added and up to 12 can be removed.

Springs

The calculated value of k_2 in the model of the TORK Damper was found to be 311N/m. This force is distributed amongst four springs, thus each spring needs a respective spring force value of 77.75 N/m or 0.44396 lbs./in. The parameters needed to achieve the desired spring rate are shown below. When designing the springs, the inner diameter must be slightly larger than the 0.25" hardened shafts that support them which led to an inner diameter of 0.272". The material was chosen to be music wire.

Parameters	***Values***
No. of active coils	17
Free length	5.5"
Wire diameter	0.019"
Outside diameter	0.31"
Spring rate	0.447 lbs./in

Exciter Design

In order to properly analyze the damping performance of the TORK Damper, it is necessary to provide sinusoidal input force over a range of frequencies. To create this type of input, an excitation device was designed. This device rotates a mass at the frequency being tested; the mass and offset distance of the center of mass can be varied to adjust the input amplitude. This excitation device was inspired by a rotational-mass testing setup used by SGRE to excite large wind turbine blades during fatigue testing. This testing setup is shown in Figure 8.

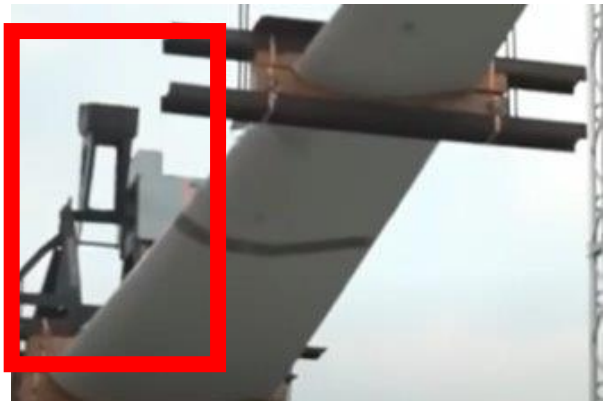

Figure 8: SGRE's excitation device used in blade fatigue testing

The requirement for the exciter is that it must be able to deflect the undamped beam's tip by ±20% of the beam's length (1.88 meters) which is equivalent to ±0.37 m. It was determined

that the forcing function needed an amplitude of $A = 1.27N$ to achieve this. For an excitation device such as this, the forcing function output by the device is described by the equation,

$$F(t) = (mr\omega^2)\sin(\omega t)$$

where m is the unbalanced mass, r is the offset distance of the center of mass of the rotating components from the center of rotation, and ω is the speed of rotation. An important concept to note about this equation is that the amplitude of the force changes as a function of ω. This means that if two tests were performed at different frequencies using the same values of m and r, the input force would not be the same between the two tests. In order to appropriately test a multitude of frequencies to ensure adequate damping, the exciter was designed with an adjustable radius for the mass and the ability to use different masses such that the force amplitude can be normalized over a range of frequency tests.

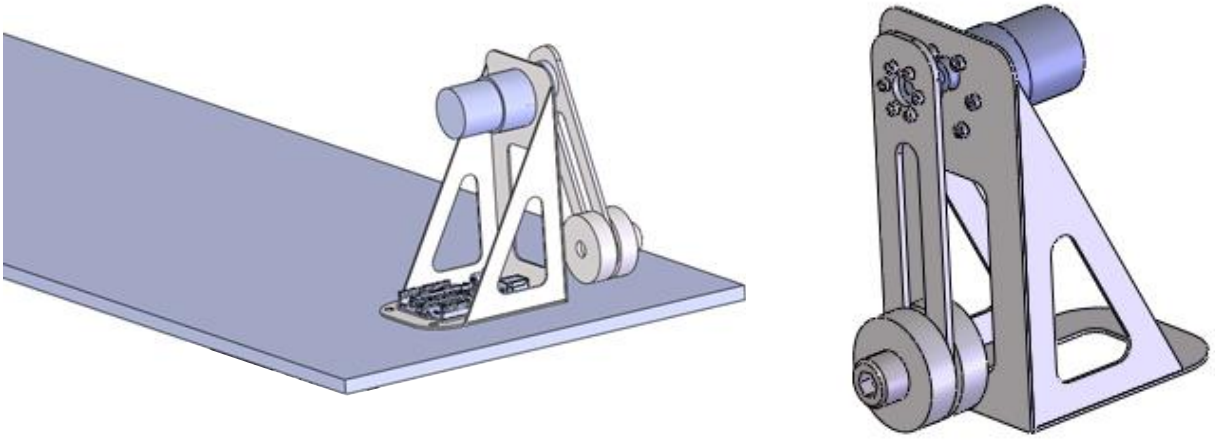

Figure 9: CAD model of the excitation device

The exciter's structure is made of welded 0.0625" steel plate with weight reducing cutouts. The motor is connected to the exciter's structure via mounting screws. The arm is connected to the motor's shaft via an aluminum universal hub. The two halves of the adjustable point mass are placed on opposing sides of the arm such that tightening the screw fixes the mass in the desired position along the slot which runs down the length of the arm. Many masses can easily be created to offer different configurable scenarios between radius and mass. A stepper motor was chosen to actuate the exciter as it is easily programmable to rotate at a certain frequency. This is because it runs under precise positional step control as opposed to using voltage control like a DC motor.

Testing

Many tests on both the component and assembly level were necessary to ensure the success of this device. Some of the tests included:

- Weighing all components
- Spring rate verification
- Load cell verification of exciter force
- Friction testing
- Natural damping of the beam
- Full assembly test

This report will expand on the most important tests at the part and assembly level – the spring rate verification test and the full assembly test.

Spring Rate Verification Test

The first test to be completed was the verification of the spring rate of the custom ordered springs. The spring rate quantifies the stiffness of a spring through the relationship between deformation distance of the spring with respect to the force applied to it. To measure this property, a test apparatus (shown in Figure 11) was designed such that a spring is placed around a shaft between a lower plate and a mock-carriage intended to hold weights. The initial distance between the base of the spring and the base of the unloaded mock-carriage was recorded and then the carriage was loaded with increasing weights and the spring length was recorded at each respective weight. The spring length was also measured as weights were removed to evaluate the possibility of static friction and hysteresis. The spring rate was evaluated at approximately 64 N/m which was 17.7% off from the initial desired spring rate of 77.75 N/m. This discrepancy is due to manufacturing tolerance. This deviation in spring rate can be accounted for with the removal of eight tungsten inserts.

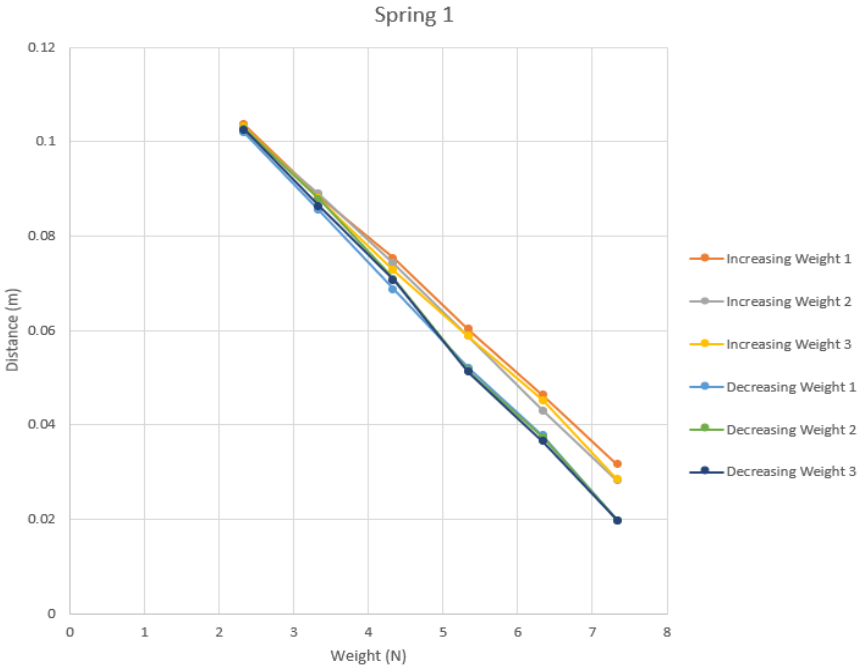

Figure 10: Spring rate verification test example result for one spring

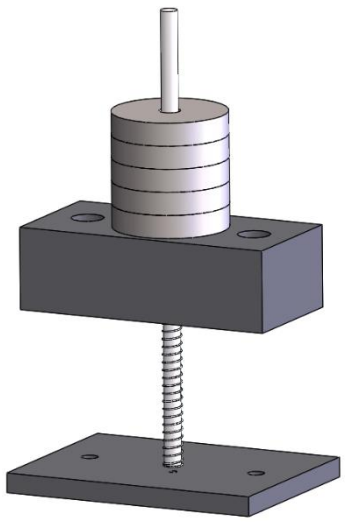

Figure 11: Spring testing apparatus

Final Testing

Introduction:

To reiterate, the purpose of the TORK Damper is to increase the damping of the beam. So, to measure the success of the damper, the damping properties of the damped beam system must be quantified. In this project, the damping properties of the system are quantified using a metric known as *logarithmic decrement*. Logarithmic decrement is related to the rate at which an underdamped system's oscillation decays after receiving an input disturbance. A higher value of logarithmic decrement corresponds to a larger amount of damping within the system. The logarithmic decrement can also be related to (and can be measured using) the steady state oscillation amplitude of the beam as a response to a constant amplitude, sinusoidal force input.

The testing method implemented measures the response of the beam to a sinusoidal input for a range of frequencies. Ultimately, this provides a magnitude of the position amplitude of the beam as it oscillates in steady state (dependent variable) as a function of input frequency (independent variable). This type of function is known as a Frequency Response Function (FRF). The maximum value within the FRF is associated with the lowest value of logarithmic decrement. The FRF of the damped beam system can be experimentally determined by measuring the steady state oscillation amplitude of the beam at many discrete input frequencies. The following sections will detail how this metric was measured.

Set Up:

A testing set up was required to accommodate the high deflection the beam must undergo (±0.37 meters or ±1.21 feet) in conjunction with the requirement that it function in multiple orientations. The consideration given to the test set up was two-fold. The test fixture needed to lift the beam high enough such that the 17 centimeter (~six inch) TORK Damper would not impact the ground. It needed to create the cantilever at the desired length on the beam and ensure that no vibration occurred behind that point (e.g. tightly clamp the beam behind the free end to simulate a fixed-end cantilever). Furthermore, the fixture had to be heavy enough to rigidly support the almost 40-pound aluminum beam representing the wind turbine blade.

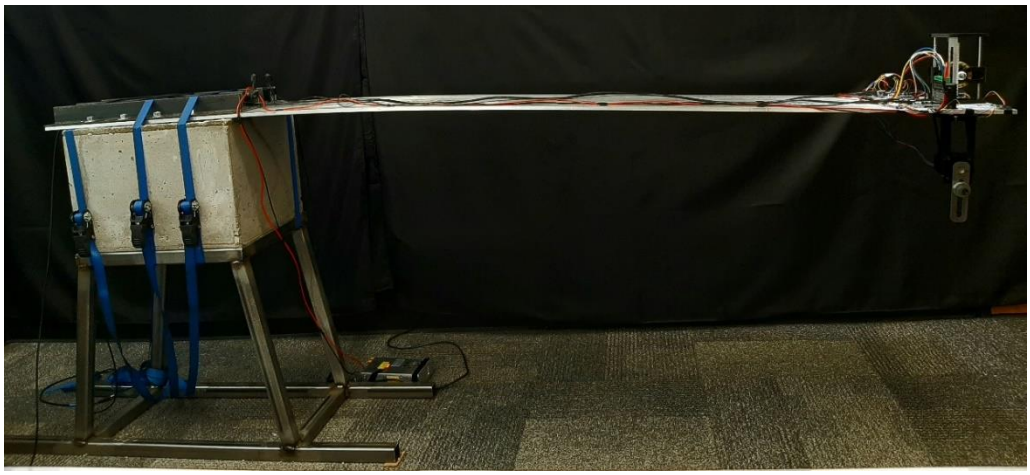

Figure 12: Full assembly testing setup (vertical TORK Damper)

To address the height requirement a steel stand was welded with long parallel feet to evenly distribute load. The steel structure stands at 23 inches tall. Atop the structure sits an approximately 275-pound concrete block that contains threaded inserts. This block is 13.25 inches tall. The fixed end of the beam has through holes that match the pattern of the threaded inserts. Six pieces of 3/16 inch 2x2 angle iron with the same set of holes run parallel on the top of the beam and are tightly secured with washers and nuts. This fixture apparatus served to create a fixed end boundary condition for the beam. The beam and concrete block are further prevented from slipping off the stand through the use of ratchet straps.

Method:

Based on the provided requirements, it was necessary to test the beam within a range of frequencies. The range of interest was determined to be between 8 and 13 radians/second (~±25% of the first natural frequency). In order to have a meaningful FRF, the input force created by the exciter must consistently be 1.27 N throughout the entire range of frequencies. As a reminder, the amplitude of force is dependent on the mass, the radius (of the center of mass), and the frequency. Since the input frequency is being changed for each test to experimentally determine the system's FRF, the radius must be varied to accommodate this change and provide a constant force amplitude.

FRFs shown in future sections are comprised of 25 tests. Each of these tests are conducted with a different input frequency (between 8 and 13 radians/second incremented by 0.2 radians/second per test) created by the exciter. Each of the 25 tests were conducted with the following procedure:

1. Set the frequency of the exciter
2. Set the radius offset of the mass on the exciter arm
3. Turn on the exciter and allow the beam to reach steady state in oscillation (approximately two minutes)
4. Measure the acceleration of the tip of beam using accelerometers and convert acceleration to position (data acquisition set up shown in Figure 14)

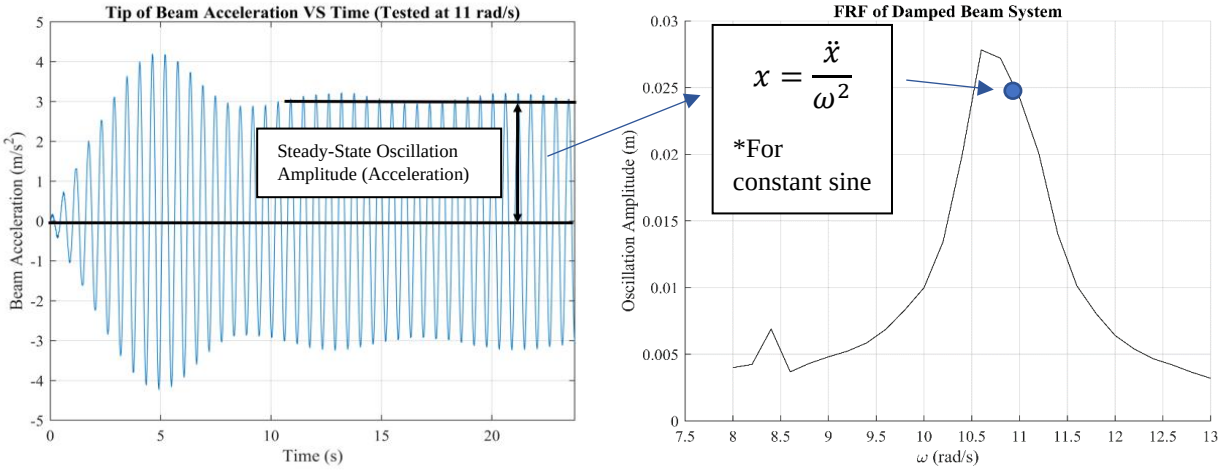

Figure 13: Graphical representation of the process to obtain one data point in the experimentally determined FRF

A graphical representation of this procedure is shown in Figure 13. One experimentally determined point on the FRF (on the right) comes from a continuous time measurement of the beam/damper system's response to a sinusoidal input force at one frequency and constant amplitude (on the left). The steady state amplitude is extracted from the acceleration vs. time data and converted to a position amplitude.

The measurement and electronics control systems included respective Arduinos to run the motor controller and accelerometers. The accelerometers were placed on each side of the tip of the beam to ensure that there was no twist occurring during deflection and to act as a redundant system to mitigate risk to data collection. Figure 14 illustrates one of the configurations of the beam's data collection set ups. In the final assembly test the exciter stand (black structure) sat on vibration isolators in order to minimize high frequency vibrations that the accelerometers were particularly sensitive to. This led to the accelerometers recording less unwanted high frequency vibrations especially at lower input frequencies.

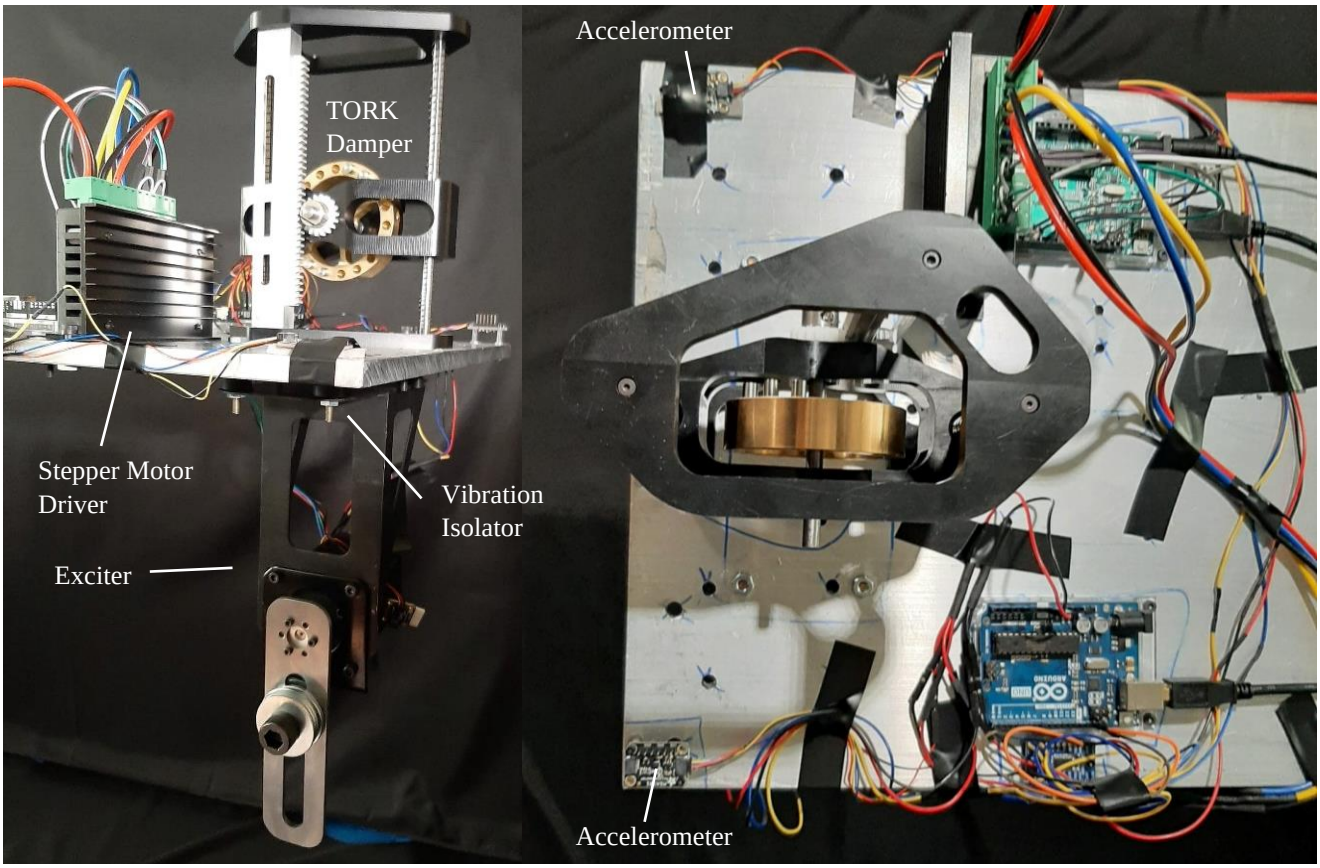

Figure 14: Beam data collection setup for full assembly testing

Another requirement for this device is that it should be able to function regardless of its orientation with respect to gravity. So, the procedure described above for experimentally determining the system's FRF was repeated with the TORK Damper vertical on the beam as well as inverted 180 degrees. Additionally, the entire beam system was rotated 90 degrees about its long axis so that the TORK Damper could be tested horizontally. The experimentally determined FRFs in these three orientations are discussed next.

Results

Ideally, the model created in SIMULINK would perfectly match the experimental FRF created with the same tuning. However, there are many small, difficult to model complexities that the real system undergoes that are outside the scope of this paper such as the force of friction and aerodynamic damping. The team is unable to perfectly model and account for every complexity. As a result, there will always be some discrepancy between reality and the model. For this reason, the model can be considered validated if the general shape and magnitudes of the model and experimental FRF match. It can be seen from Figure 15 that the data recorded using the two accelerometers on the tip of the beam closely match the theoretical model. In this case, the model matched well to the experimental results when the model and device were set to the ideal tuning of insert quantity and the TORK Damper was in the vertical orientation. When the model and device were tuned such that they *did not* contain the ideal number of inserts, the experimental results began to deviate from the model.

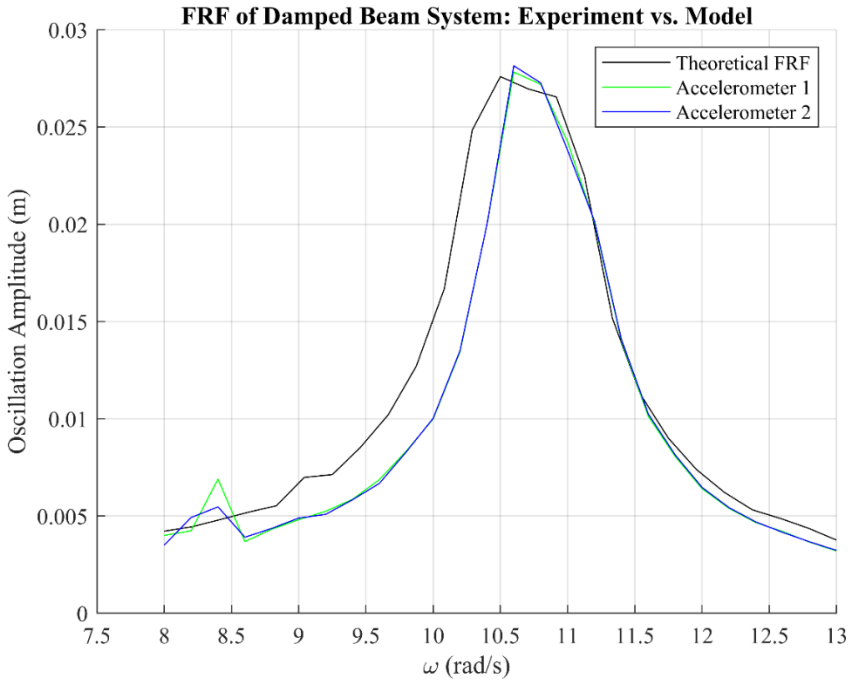

Figure 15: Comparison of modeled FRF and experimentally determined FRF of the TORK Damper

The experimentally determined FRF curves for the damped beam system in each TORK Damper orientation (vertical, inverted, and horizontal) are shown in Figure 16. To reiterate, the goal for this damping device was to increase the logarithmic decrement of damping of the cantilevered beam to at least 20% in any orientation. The logarithmic decrement values achieved for each orientation are as follows:

Orientation	***Logarithmic Decrement***
Vertical	21.00%
Inverted	18.97%
Horizontal	15.89%

Although the TORK Damper was able to meet the damping specification in the vertical orientation, it fell short of the goal in the inverted and horizontal orientations. For the inverted orientation, the team hypothesizes that the difference between the achieved value and the goal is within the measurement error of the experiment. For the horizontal orientation, however, the team hypothesizes that the underperformace is due to larger forces of friction within the TORK Damper when the beam is on its side. If the amount of friction were able to be minimized, the amplitude of the peak on the FRF would decrease as a result (meaning higher logarithmic decrement). Friction appears to be the limiting factor in the performance of the TORK Damper. Though there are many contributors to friction, a significant portion can be attributed to the interface between the linear shafts and bearings.

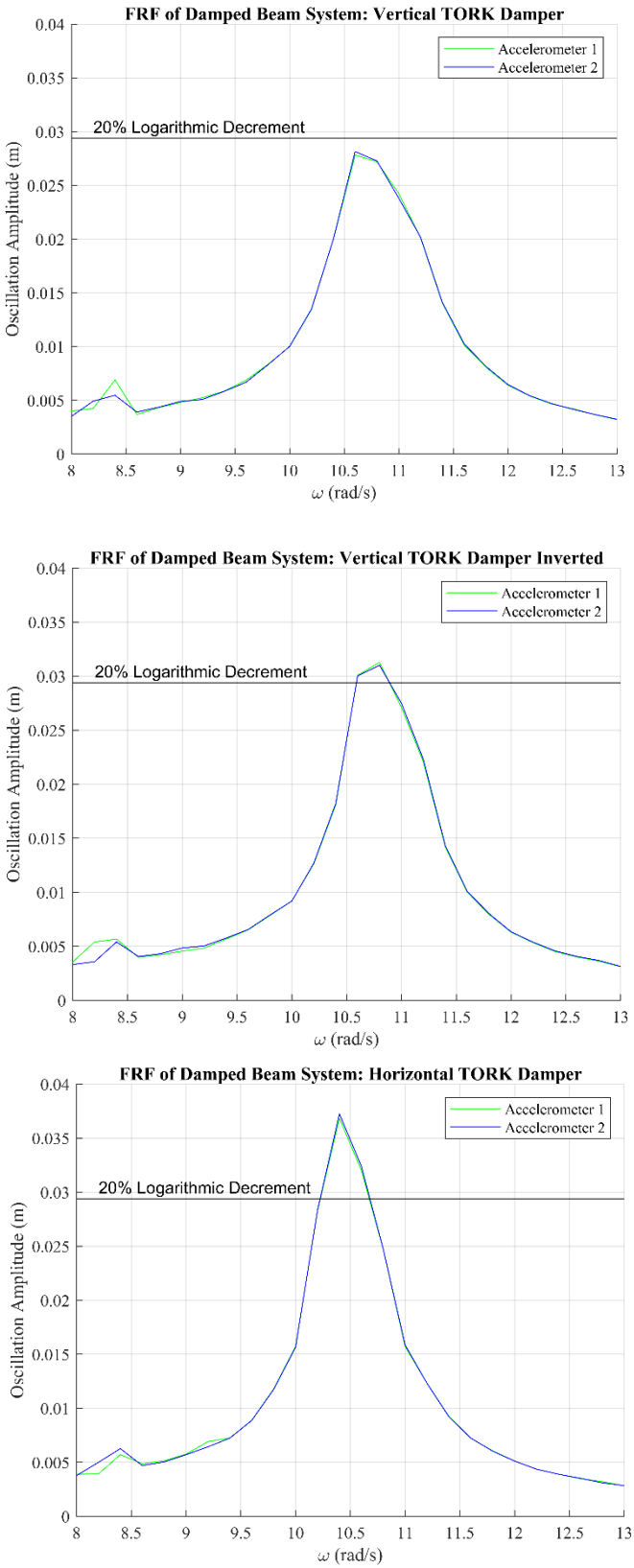

Figure 16: Experimentally determined FRFs for the TORK Damper in all three testing orientations

Conclusion

This project has shown incredible promise in terms of damping unwanted vibrations in long cantilevered beams. The TORK Damper offers its users tunable parameters that can help optimize damping and customize the device for targeted applications. Overall, the system was successfully modeled and was able to perform mostly independent of orientation. The TORK Damper achieved all of its goals within one of the three orientations but fell short in the other two. It is hypothesized that the reason the TORK Damper did not meet the required 20% logarithmic decrement specification in these two orientations was in part due to the friction forces within the system being higher than anticipated, significantly impacting the dynamics of the device. However, if the TORK Damper were to be scaled up for use in wind turbine blades, the team expects that these friction forces will become relatively less significant compared to the other forces within the system. This technology will hopefully serve to one day allow SGRE to further reduce vibrations in wind turbine blades.